Nucleic Acids Research, 2025, **53**, gkaf428
https://doi.org/10.1093/nar/gkaf428
RNA and RNA-protein complexes

Specific branches of the proteostasis network regulate the toxicity associated with mistranslation

Donovan W. McDonald[1], Rebecca N. Dib[2], Christopher De Luca[2], Ashmi Shah[3], Martin L. Duennwald[1,2,3,*]

[1]Department of Biology, The University of Western Ontario, London, ON N6A 3K7, Canada
[2]Department of Anatomy and Cell Biology, Schulich School of Medicine and Dentistry, The University of Western Ontario, London, ON N6A 3K7, Canada
[3]Department of Biochemistry, Schulich School of Medicine and Dentistry, The University of Western Ontario, London, ON N6A 3K7, Canada
[*]To whom correspondence should be addressed. Tel: +1 519 661 2111 Extension 86874; Email: martin.duennwald@schulich.uwo.ca

Abstract

All cellular functions rely on accurate protein biosynthesis. Yet, many variants of transfer RNA (tRNA) genes that induce amino acid misincorporation are found in human genomes. Mistranslation induces pleiotropic effects on proteostasis, ranging from protein misfolding to impaired protein biosynthesis and degradation. We employ *Saccharomyces cerevisiae* (budding yeast), a genetically and biochemically tractable model that facilitates quantitative analysis of how specific proteostasis pathways interact with mistranslating tRNAs. We tested two mistranslating $tRNA^{Ser}$ variants, one inducing proline to serine (P > S), the other arginine to serine (R > S) misincorporation. We found that P > S misincorporation impairs cellular fitness and sensitizes cells to protein misfolding to a greater extent than R > S misincorporation. Of note, we also show that, even though both tRNA variants induce misincorporation of serine, they result in the accumulation of misfolded proteins by distinct mechanisms. Specifically, R > S misincorporation reduces that association of Hsp70 with misfolded proteins, while P > S misincorporation impairs the degradation of nascent polypeptides. Our findings reveal that different mistranslating $tRNA^{Ser}$ variants impair specific branches of proteostasis and thus compromise cellular fitness by distinct mechanisms.

Graphical abstract

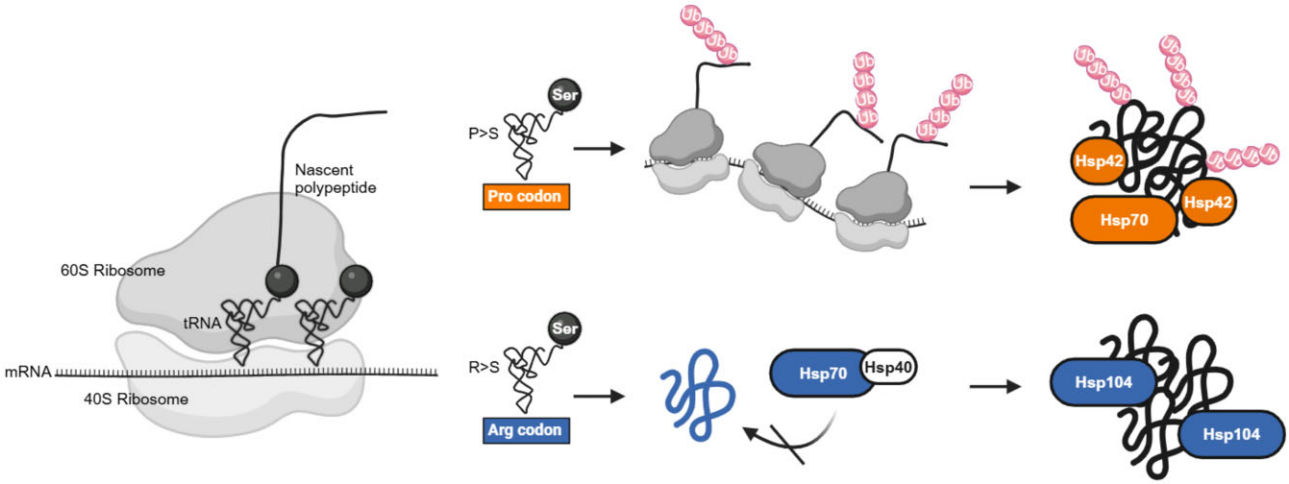

Introduction

Transfer RNAs (tRNAs) are small RNA molecules that cooperate with the ribosome to decode messenger RNA (mRNA) codons into amino acids during protein biosynthesis. tRNAs are typically between 70 and 100 nucleotides in size and share a distinctive three-hairpin loop structure, one of which contains the anticodon central to the decoding ability of tRNAs [1]. Despite the requirement for accurately synthesized proteins, cells tolerate mild levels of translation infidelity to optimize translation rates [2]. Translation infidelity, or mistranslation, refers to the inaccurate incorporation of amino acids during translation, yielding proteins that deviate from the amino

Received: February 4, 2025. **Revised:** April 16, 2025. **Editorial Decision:** April 16, 2025. **Accepted:** May 7, 2025

acid sequence dictated by the standard genetic code. Unlike most tRNAs, the aminoacyl synthetases that charge serine, alanine, leucine, and selenocysteine tRNAs do not use the anticodon sequence to discriminate tRNA identity [3]. These tRNA isotypes are thus uniquely predisposed to decoding errors due to mutations in their anticodon [4–13]. Other tRNAs can also cause mistranslation if they acquire mutations that introduce new identity elements. For example, mutations that produce a G3:U70 base pair, a potent recognition element for the alanine tRNA synthetase, can result in alanine misincorporation by non-alanine tRNAs [14, 15].

Despite their essential function, tRNA genes vary considerably within the human population [16]. While the majority of identified tRNA variants are predicted to cause loss of function, several are predicted to cause mistranslation. To assess their effects in living cells, mistranslating tRNA variants have been expressed in several model organisms, including yeast [4, 5, 11, 13, 17], cultured mammalian cells [7, 14, 18–21], fruit flies [9, 10], zebrafish [8], mouse models [6], and chick embryos [22]. In all these systems, expression of mistranslating tRNA variants promotes drastically variable rates of mistranslation, toxicity, and possibly impair different cellular pathways. Furthermore, differences in cell types, organisms, the frequency of mistranslation, the specific amino acid substitution produced, and even the specific mistranslated codon may determine their effects on cellular functions and survival [9, 12, 13].

Due to the direct effect of mistranslation on protein structure and function, mistranslation is often postulated to interfere with protein homeostasis (proteostasis) by producing mismade proteins that cannot attain their proper 3D conformation, i.e. misfold. In zebrafish and cultured human cells, mistranslating tRNA variants cause the accumulation of polyubiquitinated proteins, induce protein aggregation, and induce stress response pathways [7, 8]. In yeast, constitutive expression of mistranslating $tRNA^{Ser}$ variants induces modest levels of mistranslation, stunts cellular growth, activates stress responses, impairs protein biosynthesis, and can induce aggregation of metastable proteins [4, 11, 15]. Also, expression of inducible mistranslating $tRNA^{Ser}$ variants potentiates higher rates of mistranslation (~12%), exacerbates the growth defect, and induces a robust heat shock response [23]. In addition, mistranslation caused by errors in tRNA editing induces aggregation of proteins [24]. Whether mistranslated proteins cause cellular toxicity by inducing misfolding and aggregation, or whether mistranslated proteins impair proteostasis by sequestering protein quality control machinery, or a combination of both, remains unclear.

Proteostasis describes all cellular functions that regulate the proper production, maintenance, and degradation of proteins, thereby safeguarding accurate protein folding and preventing the accumulation of misfolded proteins [25]. Molecular chaperones and heat shock proteins bind misfolded proteins and either refold them into functional conformations or triage them for degradation by the proteasome or autophagy [26, 27]. Protein misfolding stress, such as heat shock, can lead to the accumulation of misfolded proteins and the concomitant induction of the heat shock response [28, 29]. Activation of Hsf1, the major heat shock transcription factor in eukaryotic cells, increases the expression of many different proteostasis-related genes during heat shock, which promotes cellular survival by either refolding or degrading misfolded proteins [25, 28, 29]. Yet even under permissive conditions, chaperones are required for efficient *de novo* translation of proteins and help to regulate their maturation, including their folding, complex formation, localization, and degradation [30–32].

Impairment of proteostasis can be detrimental to cellular function and survival and is linked to a bevvy of protein misfolding diseases, notably neurodegenerative diseases [25]. We hypothesize that mistranslation induces protein misfolding and, accordingly, cellular toxicity. Here, we specifically investigate how mistranslating $tRNA^{Ser}$ variants impair proteostasis. We explore two distinct mistranslating $tRNA^{Ser}$ variants that induce either proline to serine (P > S) or arginine to serine (R > S) misincorporation. We show that both mistranslating $tRNA^{Ser}$ variants induce accumulation of misfolded proteins, albeit through distinct mechanisms. We find that expression of a R > S mistranslating $tRNA^{Ser}$ decreases association of Hsp70 with misfolded proteins, potentially due to impaired interactions between Hsp70 and misfolded proteins containing R > S substitutions. By contrast, expression of a P > S mistranslating $tRNA^{Ser}$ variant induces accumulation of polyubiquitinated but detergent-soluble nascent polypeptides, indicating that degradation of misfolded nascent proteins is impaired by P > S misincorporation. By providing a genetic link between P > S misincorporation and co-translational proteostasis, we illustrate the importance of translation fidelity in triaging newly synthesized proteins. Moreover, our results document that the expression of different mistranslating $tRNA^{Ser}$ variants distinctly interact with different branches of the proteostasis network. Our results therefore contribute to a nuanced understanding of how different types of mistranslation can impair proteostasis, thereby contributing to cellular toxicity and possibly to human diseases by distinct mechanisms.

Materials and methods

Yeast strains, media, and plasmids

Yeast strains

All yeast strains are derivatives of the wild-type haploid BY4742, W303, or DS10 strains (Supplementary Table S1). Three W303 strains containing mutant HSF1 alleles (W303 *Δhsf1*::KANMX HSF1:TRP1 4×HSE-YFP:LEU2, W303 *Δhsf1*::KANMX *hsf1ΔN*:TRP1 4×HSE-YFP:LEU2, and W303 *Δhsf1*::KANMX *hsf1ΔC*:TRP1 4×HSE-YFP:LEU2) were generously provided by Dr David Pincus [29]. The W303 *Δire1* strain [33], the W303 *Δhsp104* and W303 *Δhsp104Δhsp42Δhsp26* strains [34], and the W303 *Δsti1* and *Δaha1* strains [35] were described previously. The W303 *Δssa1–4* TEFp SSA1 strain and the DS10 *Δssz1*, *Δssb1Δssb2*, and *Δssz1Δssb1Δssb2* strains were kind gifts from Dr Elizabeth Craig [36, 37]. We received the BY4741 *Δnac* strain from Dr Elke Deuerling [38]. All other strains were acquired from the yeast knockout collection [39], the yeast GFP clone collection [40], or the yeast decreased abundance by mRNA perturbation (DAmP) collection [41].

Growth conditions

All strains were grown on yeast-peptone-dextrose agar plates for 2 days at 30°C before cells were used for transformations. For ectopic expression of tRNA variants or other protein encoding genes, cells were transformed with plasmid DNA using the standard LiAc-PEG protocol [42]. All cells were grown using synthetic defined (SD) media

supplemented with 2% glucose, 6.7 g/L yeast nitrogenous bases with ammonium sulfate, and amino acids (40 mg/L L-lysine, 20 mg/L L-arginine, 10 mg/L L-threonine, 60 mg/L L-phenylalanine, 20 mg/L L-isoleucine, 10 mg/L L-methionine, and 20 mg/L adenine hemisulfate). Media were supplemented with additional amino acids for selection where necessary (20 mg/L L-histidine, 60 mg/L L-leucine, 20 mg/L uracil, and 80 mg/L L-tryptophan). For all experiments, cells were first grown overnight in liquid SD media at 30°C with agitation. Cells were plated on SD agar plates containing 2% glucose and supplemented with small molecules where indicated.

Plasmids

All plasmids used in this study are described in Supplementary Table S2. tRNA variants were expressed using plasmids obtained from Dr. Christopher J. Brandl (pSUP17-wt, pSUP17-P > S_{weak}, pSUP17-P > S_{strong}, and pSUP17-R > S) [5]. For co-expression experiments, tRNA encoding fragments were excised from pSUP17 plasmids using *Eco*RI-*Hin*dIII and were subsequently ligated into pRSII314 backbone [43] to generate p314-SUP17-wt, p314-SUP17-P > S_{weak}, p314-SUP17-P > S_{strong}, and p314-SUP17-R > S. The Hsp104-YFP aggregation reporter was generated using gateway cloning to produce p415 GPD HSP104-YFP.

Growth assay

To measure differences in cellular growth, we performed spotting assays as described in Petropavlovskiy *et al.* [44]. In summary, cells were grown overnight in SD media and diluted to $OD_{600} = 1$ in a 96-well plate. Five-fold serial dilutions were prepared using 96-well plates and the cells were then spotted onto SD agar plates supplemented with 2% glucose and small molecules where indicated. Plates were then incubated in a humidified incubator at either 30°C or 37°C for 24–72 h. After sufficient cell growth, plates were photographed for downstream analysis using Fiji [45]. *Δpdr5* cells were used for treatments with MG-132. The densitometry of spots at the same dilution factor was compared with control cells to assess changes in cellular growth. At least three independent biological replicates were used for each sample.

Heat shock response reporter and flow cytometry

To assess transcriptional regulation of the heat shock response, we utilized a fluorescence-based heat shock response reporter system, 4×HSE-YFP [29]. Briefly, we grew cells expressing 4×HSE-YFP overnight in SD media. We pelleted cells that were in mid-log phase and resuspended them in phosphate-buffered saline. We then performed flow cytometry using the BD Bioscience FACS Celesta flow cytometer. A 488 nm laser was used to assess the fluorescence intensity of YFP per cell for a total of 150 000 cells per replicate. No gating was performed. Three independent experiments were conducted, and the median fluorescence intensity was recorded for each replicate.

Protein extraction and western blot

Liquid cell cultures were lysed using a standard alkaline lysis protocol [46]. Briefly, cells were resuspended in 100 mM NaOH, 2% sodium dodecyl sulfate (SDS), 50 mM Ethylenediaminetetraacetic acid (EDTA), and 2% 2-mercaptoethanol, boiled for 5 min, diluted in 1× Laemmli buffer and boiled again for 5 min. Cell lysates were then resolved by sodium dodecyl sulfate–polyacrylamide gel electrophoresis (SDS–PAGE), after which proteins were transferred to a polyvinylidene fluoride (PVDF) membrane. Membranes were then washed with 0.1% Tween 20 in Tris buffered saline (TBST) and blocked in 5% skim milk before being incubated in primary antibody overnight at 4°C with agitation. Primary antibodies used to target Hsp104 (Rb anti-Hsp104, 1:5000), Hsp42 (Rb anti-Hsp42, 1:5000), and Hsp26 (Rb anti-Hsp26, 1:5000) were kindly gifted to us by Dr Johannes Buchner. Primary antibodies used to target Hsp70 (Ms anti-Hsp70, 1:1000; Thermofisher, MA3-006), puromycin (Ms anti-puromycin, 1:500; Sigma, MABE343), ubiquitin (Rb anti-ubiquitin, 1:1000; R&D Systems, MAB8595), and the loading control Pgk1 (Rb anti-Pgk1, 1:5000; Origene, AP21371AF-N) were obtained commercially. Membranes were then washed in TBST and incubated in secondary antibodies conjugated with AlexaFluor680 at 1:5000 dilution (Thermofisher, A32734/A10038) for 1 h before being imaged using the ChemiDoc MP (Bio-Rad). Images were then analyzed using Fiji to measure densitometry. Where noted, *Δpdr5* cells were treated with 50 μM MG-132 for 6 h before lysis.

Gene ontology (GO) term and transcription factor enrichment analysis of transcriptomics dataset

FASTQ files with RNA sequencing data from cells expressing either vector control, P > S strong, or R > S were acquired from NCBI Gene Expression Omnibus series accession number GSE174145 [13]. Reads were trimmed, counted, and analyzed as described in Berg *et al.* [13]. YEASTRACT+ [47] was used to assess enriched GO terms and enriched transcription factors for the full set of genes upregulated 0.5-fold (Benjamini–Hochberg-adjusted *P*-value <.05) for cells expressing either P > S strong or R > S. Briefly, the rank by GO tool was used to assess enriched GO terms, with ontology set to biological processes and a cutoff of *P*-value <.001. The rank by TF tool was used to assess enriched transcription factors, considering either expression or DNA binding evidence, only considering transcription factors acting as activators and a cutoff of *P*-value <.001.

Fluorescence microscopy and foci analysis

Microscopy

To assess protein aggregation in living cells, we used cells expressing Hsp104-YFP [24]. Cells were grown to mid-log phase and then imaged with either the Zeiss Axio Vert.A1 (Carl Zeiss™) or the BioTek Cytation 5 Cell Imaging Multi-mode Reader (Agilent) using a 20× objective and bright field and GFP filter sets. Three separate fields of view were imaged for each sample and each experiment was repeated three times, for a total of nine images per sample.

Analysis of fluorescent foci

The number of Hsp104-YFP foci per cell was assessed in R using the EBImage library [48]. Briefly, the total number of cells in each image was determined by setting a low intensity threshold to highlight all fluorescent signals. The total number of foci was assessed in each image by setting a high intensity threshold that only highlights the high fluorescent intensity fluorescent signals. R script used to analyze foci is available at https://doi.org/10.6084/m9.figshare.28688966.

Sedimentation of insoluble proteins

Sedimentation assay

Liquid cell cultures were harvested and resuspended in 100 mM Tris (pH 7.5), 200 mM NaCl, 5% glycerol, 1× ProBlock Gold Yeast/Fungi Protease Inhibitor Cocktail (GoldBio, GB-333-1), 50 mM EDTA, and 1 mM dithiothreitol (DTT). An equal volume of acid washed glass beads (Sigma, G8772) was added to the cell suspension and the cells were disrupted using the Analog Disruptor Genie (Scientific Industries, SI-D238) for five 60-s intervals interspersed with 60-s incubations on ice. The lysate was separated from the beads and the protein concentration was measured using the Pierce BCA Protein Assay Kit (Thermofisher, 23225). An aliquot of the total protein was transferred to a new tube and the remaining lysate was sedimented at 500 × *g* for 15 min at 4°C. The supernatant was collected and the pellet was resuspended in an equal volume of lysis buffer. All fractions were diluted in 2× SUMEB [1% SDS, 8 M urea, 10 mM MOPS (pH 6.8), 10 mM EDTA, 0.01% bromophenol blue] and used for western blotting to detect Hsp70, Hsp104, and Hsp42.

Triton X-100 solubility assay

Cells were lysed as described above. Insoluble proteins were then pelleted at 16 000 × *g* for 20 min at 4°C. The supernatant was discarded, and the pellet was then resuspended in 2% Triton X-100, 100 mM Tris (pH 7.5), 200 mM NaCl, and 1× ProBlock Gold Yeast/Fungi Protease Inhibitor Cocktail. Samples were then disrupted for 30 s using the Analog Disruptor Genie. The Triton X-100 insoluble proteins were then pelleted at 16 000 × *g* for 20 min at 4°C. The supernatant (Triton X-100 soluble proteins) was collected and diluted in 1× SUMEB. The pellet (Triton X-100 insoluble proteins) was resuspended in an equal volume of lysis buffer without protease inhibitors and then diluted in 1× SUMEB. Both the Triton X-100-soluble and the -insoluble fractions were resolved using SDS–PAGEs. After resolution, the total proteins were stained in the SDS-PAGE with Coomassie or the proteins were transferred to PVDF membranes and western blots were performed for detection of polyubiquitinated proteins, Hsp104, Hsp70, and Hsp42. Both the Coomassie stained gel and the western blot images were analyzed using Fiji [45] to quantify the ratio of Triton X-100 soluble to insoluble proteins by densitometry.

Click chemistry labelling of nascent polypeptides

Nascent polypeptides were labelled using click chemistry as described previously [49]. To label nascent polypeptides, liquid cell cultures were resuspended in media lacking methionine and containing 50 μM L-azidohomoalanine (AHA) for 5 min. Cells were then pelleted and resuspended in fresh media lacking AHA and containing methionine for a time course of 30 min. After 0, 15, and 30 min, cells were harvested and lysed using a standard alkaline lysis protocol as previously described. To assess solubility of nascent polypeptides, cells were treated with AHA for 5 mins, lysed with glass beads, and Triton X-100 soluble and insoluble proteins were fractionated as described previously. AHA-labelled peptides were then labelled with 10 μM sDIBO alkyne AlexaFluor488 overnight at room temperature. Labelling was repeated using lysates extracted from samples that were not treated with AHA as a control. Lysates were then resolved by SDS–PAGE and the SDS–PAGE was then stained with Coomassie to stain total proteins. Fluorescently labelled and Coomassie-stained proteins were imaged using the ChemiDoc MP and images were further analyzed using Fiji.

Puromycin labelling of nascent polypeptides and immunoprecipitation

Puromycin labelling and western blot

To label nascent polypeptides, liquid cultures of *Δpdr5* cells were resuspended in liquid media containing 500 μM puromycin for 5 min. Cells were then either immediately harvested for lysis or were resuspended in media lacking puromycin for 5 min before being harvested for lysis. For assessment of the levels or puromycin-labelled nascent polypeptides, cells were lysed using a standard alkaline lysis protocol as previously described. Lysates were then resolved by SDS–PAGE, and western blots were performed targeting puromycin and the loading control Pgk1.

Immunoprecipitation of puromycin-labelled nascent polypeptides

For assessment of the ubiquitination of puromycin-labelled nascent polypeptides, we immunoprecipitated the puromycin-labelled nascent polypeptides. After puromycin treatment, cells were harvested, resuspended in 10 mM Tris (pH 7.5), 100 mM NaCl, 30 mM $MgCl_2$, 0.1% NP-40, and 1× ProBlock Gold Yeast/Fungi Protease Inhibitor Cocktail (GoldBio, GB-333-1), and disrupted by glass beads as described previously. The lysate was separated from the beads and centrifuged at 16 000 × *g* for 20 min. The supernatant was transferred to a fresh tube and the protein concentration was measured using the Pierce BCA Protein Assay Kit. After lysis, 1 μg of protein was diluted to 500 μl with lysis buffer to be used for the immunoprecipitation. A total of 50 μl of protein was aliquoted into a new tube and diluted (1:5) in lysis buffer and 1× Laemmli buffer to use as the input control. To clear the lysate, 30 μl of magnetic beads coupled to protein G were pelleted and resuspended twice in 50 μl lysis buffer before being added to the remaining protein and incubated for 1 h at room temperature with gentle end-over-end rotation. The beads were then magnetized and anti-puromycin antibody (Ms anti-puromycin, 1:50; Sigma, MABE343) was added to the remaining sample. The sample was incubated overnight at 4°C with gentle end-over end rotation. The lysate was then incubated with 30 μl of magnetic beads coupled with protein G, washed, and resuspended in 50 μl of lysis buffer, for 1 h at room temperature with gentle rotation. Beads were then magnetized, washed twice with PBST, and proteins were eluted in 60 μl of lysis buffer containing 1× Laemmli buffer. The immunoprecipitation protocol was also performed using untreated cells and anti-puromycin antibody alone as controls. Total and immunoprecipitated proteins were resolved by SDS–PAGE, and western blots were performed targeting puromycin, ubiquitin, and the loading control Pgk1. For immunoprecipitated proteins, VeriBlot for IP Detection Reagent (1:1000; abcam, ab131366) was used in place of secondary antibody for detection. Western blots were imaged using the ChemiDoc MP and images were analyzed using Fiji.

Results

Mistranslating tRNA^{Ser} variants sensitize cells to protein misfolding stress

Mistranslating tRNA^{Ser} variants can impair cellular fitness, activate stress responses, cause protein misfolding, and even impair protein biosynthesis [4, 5, 8, 11, 19, 21, 22]. Different types of mistranslation induce stress in cells, likely through different mechanisms [9, 12, 13]. Previous reports established that mistranslating tRNA^{Ser} variants that induce P > S and R > S misincorporation both impair growth and activate Hsf1, the major transcriptional regulator of the heat shock response [4, 5, 13]. However, the specific mechanisms through which these mistranslating tRNA^{Ser} variants impose stress on the cell and to what extent different mistranslating tRNA variants elicit cellular stress and reduce cellular fitness remain unclear. We employ a yeast model best suited to investigate these specific mechanisms through a combination of complementary genetic and biochemical assays. To induce mistranslation in yeast cells, we utilize previously described mistranslating variants of the yeast serine tRNA SUP17 (Fig. 1A) [5, 13]. Briefly, two SUP17 variants (P > S weak and P > S strong) induce misincorporation of serine instead of proline residues and contain secondary mutations (G9A in P > S weak and G26A in P > S strong) that reduce the rate of mistranslation to ~0.5% and 5%, respectively [5]. The third SUP17 variant (R > S) we explore here, which induces misincorporation of serine instead of arginine residues and contains the G26A mutation, yields a rate of misincorporation of ~3.5% [13].

We first assessed whether mistranslating tRNA^{Ser} variants sensitize cells to protein misfolding stress. We performed growth assays using cells deleted for the multidrug transporter PDR5 (*Δpdr5*) and transformed with either vector control or plasmids encoding SUP17 (wt tSer), P > S weak, P > S strong, or R > S. We observed that cells expressing P > S strong exhibit a strong growth defect, as has been previously described (Fig. 1B). In addition, we demonstrate that cells expressing P > S strong are more sensitive than control cells to both exposure to elevated temperature (37°C), treatment with the proteasome inhibitor MG-132, and treatment with the Hsp90 inhibitor radicicol (Fig. 1B and D). In contrast, expression of R > S only induced a modest growth defect and, unlike P > S strong, did not sensitize cells to stress caused by elevated temperature, treatment with MG-132, or treatment with radicicol (Fig. 1C and D).

Next, we tested whether mistranslating tRNA^{Ser} variants impair recovery from stress. We exposed cells expressing mistranslating tRNA^{Ser} variants to elevated temperature (37°C) for 24 h or a heat shock (42°C) for 1, 2, or 3 h. We then tested their ability to regrow at 30°C. While 24-h exposure to 37°C did not change the fitness of cells expressing P > S strong, a 1-h heat shock at 42°C was sufficient to impair the fitness of cells expressing P > S strong (Fig. 1E). In contrast, exposure to 37°C for 24 h did impair the fitness of cells expressing R > S (Fig. 1F). While a heat shock at 42°C for 1 h was insufficient to impair the fitness of cells expressing R > S, extending the heat shock for 2 or 3 h did exacerbate the growth defect of cells expressing R > S compared with control cells (Fig. 1F). We also document that the stress sensitivity caused by both types of serine misincorporation is specific to stressors that induce misfolding of cytosolic and nuclear proteins, as neither type of serine misincorporation sensitized cells to ER stress (tunicamycin or DTT) or oxidative stress (H_2O_2 and diamide) (Supplementary Fig. S1).

Previous studies indicate that P > S and R > S mistranslating tRNA variants activate Hsf1 [5, 13], yet the extent of increased expression of Hsf1-regulated genes and other cellular stress responses and proteostasis-associated genes, remained unclear. We assessed enriched GO terms and transcription factors associated with upregulated genes from publicly available transcriptomics datasets of cells expressing P > S strong or R > S. Although both P > S strong and R > S induce upregulation of genes associated with overlapping proteostasis related processes, such as cellular response to heat, chaperone co-factor dependent protein refolding, and proteolysis, P > S strong showed a greater enrichment in each of these GO terms, confirming that P > S strong induces a more robust activation of the heat shock response than R > S (Supplementary Fig. S2D). Furthermore, P > S strong also induced upregulation of genes associated with other proteostasis-related processes, such as response to hydrogen peroxide and protein stabilization (Supplementary Fig. S2D). Both P > S strong and R > S induce sets of upregulated of genes that are enriched for genes regulated by overlapping stress induced transcription factors, including Hsf1, Hac1 (regulator the unfolded protein response), Msn2, and Msn4 (regulators of the general stress response) (Supplementary Fig. S2E). We again observed that P > S strong induced a greater enrichment of each of genes controlled by these stress induced transcription factors than R > S (Supplementary Fig. S2E).

We next investigated whether P > S and R > S misincorporation induce increased steady state levels of molecular chaperones via western blot as these plausibly directly interact with mistranslated proteins. Although both types of serine misincorporation induced increased steady state levels of Hsp104, Ssa1-GFP, and Hsp42, we again discovered that P > S misincorporation induces a greater increase in all of these chaperones than R > S misincorporation (Fig. 1G–L).

In sum, we reveal that P > S and R > S misincorporation both induce growth defects and sensitize cells to conditions that induce the accumulation of misfolded proteins in the cytoplasm and nucleus. Of note, we illustrate that cells do not respond identically to these two mistranslation events, where P > S misincorporation induces a stronger growth defect and greater sensitivity to cytosolic and nuclear protein misfolding stress than R > S misincorporation. The stronger growth defect caused by P > S misincorporation also corresponds to a more robust induction of the heat shock response when compared with R > S misincorporation.

The cytosolic Hsp70 family primarily mitigates the toxic effects of R > S misincorporation

Molecular chaperones are the primary defense mechanism cells use to refold misfolded proteins [50]. Although several studies indicate mistranslation induces protein misfolding [8, 11, 24], the specific mechanisms that cells use to tolerance protein misfolding is enigmatic. To answer such a complex question, we took a quantitative approach to interrogate genetic interactions between Hsf1, molecular chaperone systems, and serine misincorporation in the yeast model using simple but reliable growth assessment.

First, we altered molecular chaperone and heat shock protein expression by employing yeast strains that express different variants of Hsf1: wild-type Hsf1, the constitutively

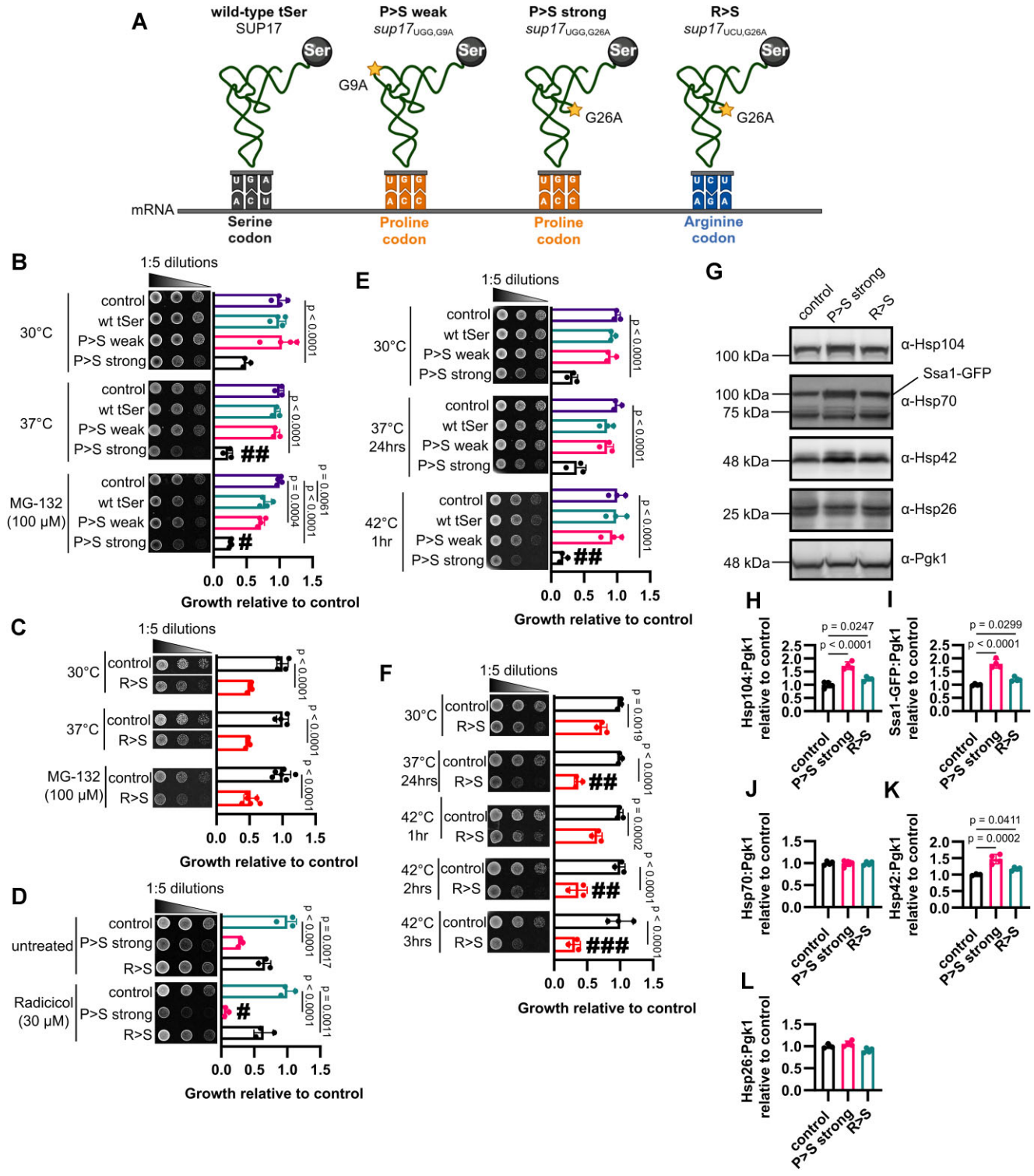

Figure 1. P > S misincorporation impairs proteostasis to a greater extent than R > S misincorporation. (**A**) Schematic of SUP17 variants used in this study. (**B**) Growth assays of cells expressing either vector control, wild-type SUP17 (wt tSer), or the SUP17 variants P > S weak or P > S strong 30°C, 37°C or at 30°C using plates supplemented with MG-132. (**C**) Growth assays of cells expressing either vector control or the SUP17 variant R > S 30°C, 37°C or at 30°C using plates supplemented with MG-132. (**D**) Growth assays of cells expressing either vector control, P > S strong, or R > S using plates supplemented with radicicol. (**E**) Growth assays of cells expressing either vector control, wt tSer, P > S weak, or P > S strong pre-incubated at 37°C for 24 h or 42°C for 1 h. (**F**) Growth assays of cells expressing either vector control or R > S were pre-incubated at 37°C for 24 h or 42°C for 1, 2, or 3 h. All plates were incubated for a period of 24–72 h before being imaged and analyzed. (**G**) Western blots and quantification (**H**–**L**) of lysates from cells expressing either vector control, P > S strong or R > S. The means (±SD) are represented graphically for at least three independent experiments. # Symbols indicate significant differences compared with cells expressing the same tRNA variants in control conditions (#$P < .05$; ##$P < .01$; ###$P < .001$).

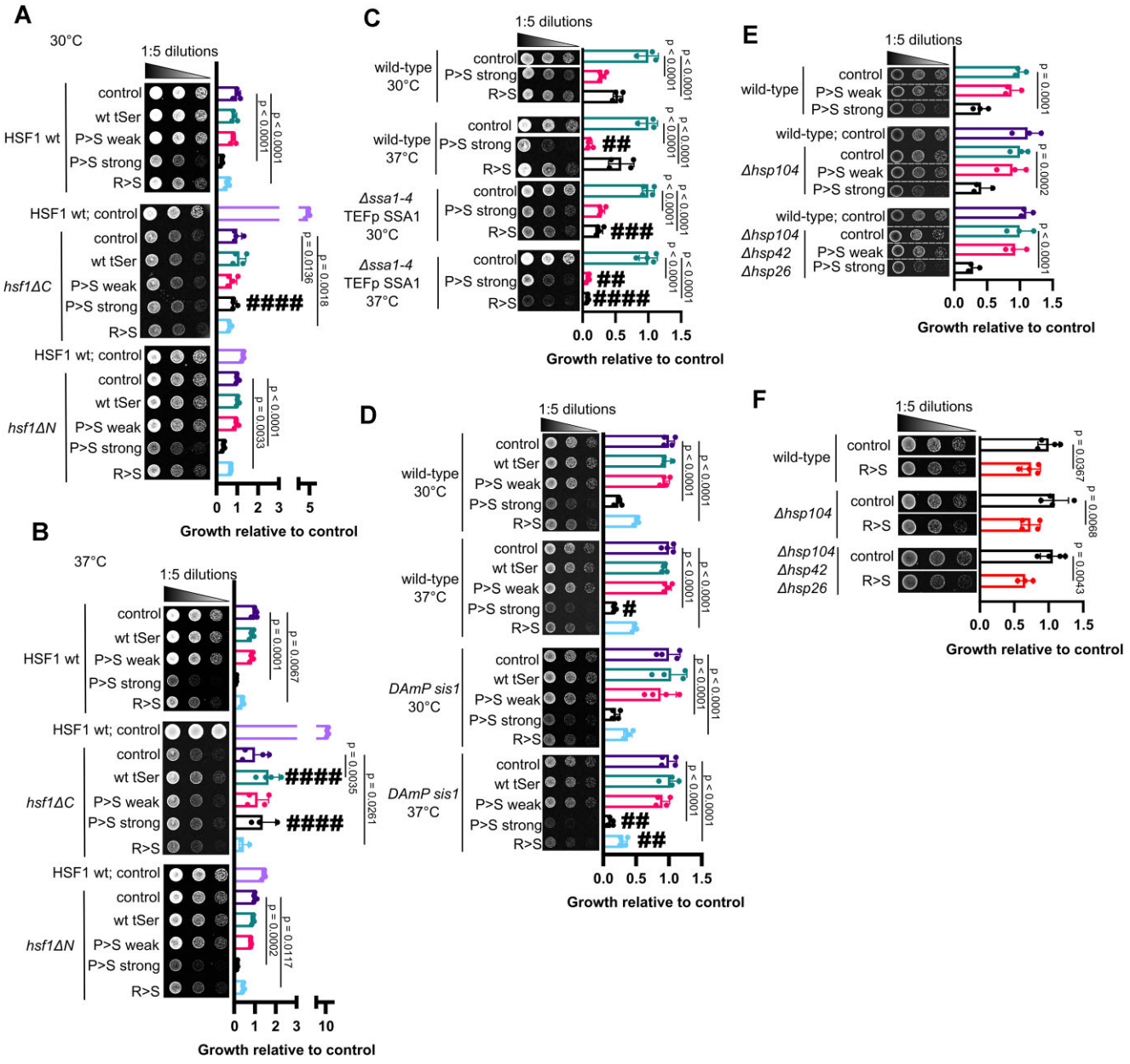

Figure 2. The cytosolic Hsp70s predominantly regulate the fitness of cells with R > S misincorporation. Growth assay using cells expressing wild-type Hsf1 (HSF1 wt), the inhibited *hsf1ΔC*, or the constitutively active *hsf1ΔN* and expressing either vector control, SUP17 (wt tSer), or the mistranslating $tRNA^{Ser}$ variants P > S weak, P > S strong, or R > S at (**A**) 30°C or (**B**) 37°C. (**C**) Growth assays using cells deleted for SSA1, SSA2, SSA3, and SSA4 (*Δssa1–4*) complemented by a plasmid encoding a single copy of SSA1 (*Δssa1–4* p416 TEF SSA1) and expressing either vector control, P > S strong, or R > S at 30°C or 37°C. (**D**) Growth assays with *DAmP sis1* cells expressing either vector control, wt tSer, P > S weak, P > S strong, or R > S at 30°C or 37°C. (**E**) Growth assays with *Δhsp104* and *Δhsp104 Δhsp42* Δhsp26 cells expressing either vector control, P > S weak, or P > S strong. (**F**) Growth assays with *Δhsp104* and *Δhsp104 Δhsp42* Δhsp26 cells expressing either vector control or R > S. The mean growth (±SD) relative to vector control are represented graphically for at least three independent experiments. # Symbols indicate significant differences compared with wild-type cells expressing the same tRNA variant at 30°C (*#P* < .05; *##P* < .01; *###P* < .001; *####P* < .0001).

activated *hsf1ΔN*, or the inhibited *hsf1ΔC* [29]. We first established that *hsf1ΔN* increases Hsf1 activity in cells expressing mistranslating $tRNA^{Ser}$ variants, while expression of *hsf1ΔC* impairs Hsf1 activity in cells expressing mistranslating $tRNA^{Ser}$ variants (Supplementary Fig. S3). Our growth assays demonstrate that constitutive Hsf1 activation is insufficient to improve fitness of cells expressing mistranslating $tRNA^{Ser}$ variants as *hsf1ΔN* had no effect on fitness of cells expressing P > S strong or R > S when compared with control cells, even when subjected to elevated temperature (Fig. 2A). Furthermore, impairing Hsf1 signaling by expressing *hsf1ΔC* surprisingly improved the fitness of cells expressing P > S strong, but not R > S, when compared with control cells (Fig. 2A and B). We also found that other stress responses are not involved in tolerance of P > S and R > S misincorporation. Specifically, we tested cells with inhibited general stress response due to deletions of either, MSN2 (*Δmsn2*) or MSN4 (*Δmsn4*) and cell with inhibited unfolded protein response by

deleting IRE1 (*Δire1*). Neither loss of Ire1, Msn2, nor Msn4 changed fitness of cells expressing P > S strong and R > S (Supplementary Fig. S4).

Because we found that Hsf1 induction is dispensable for tolerance of P > S and R > S misincorporation, we speculated that constitutively expressed molecular chaperones, rather than stress-induced molecular chaperones, predominantly manage mistranslated peptides. We first assessed the Hsp70 chaperone system. To impair Hsp70 function, we took advantage of a yeast strain with drastically reduced Hsp70 expression, i.e. a strain deleted for all four alleles encoding cytosolic Hsp70s (*Δssa1–4*) complemented with a plasmid encoding one copy of SSA1 expressed under the constitutive TEF promoter [36]. Our data indicate that reduced abundance of Hsp70 exacerbates the growth defect associated with R > S, but not P > S strong, in cells grown at 30°C and, to a much greater extent, at 37°C (Fig. 2C). We then assessed whether Sis1, a J protein and major regulator of cytosolic Hsp70, is involved in tolerance of mistranslating $tRNA^{Ser}$ variants. We performed growth assays using a strain expressing a DAmP allele of SIS1 (*DAmP sis1*) and show that reduced Sis1 expression only exacerbates growth defect associated R > S in cells exposed to elevated temperature (Fig. 2D). We demonstrate that interactions between impaired function of the cytosolic Hsp70 and serine misincorporation are highly specific to R > S misincorporation, as deletion of other Hsp70 co-chaperones (*Δsse1*, *Δhlj1*, and *Δydj1*) also do not exacerbate the growth defect associated with P > S strong (Supplementary Fig. S5A). Furthermore, our data reveal that other cytosolic chaperone and proteostasis systems are not implicated in tolerance of P > S misincorporation, as genetic impairment of the Hsp90 system (Supplementary Fig. S5B and C) and the ubiquitin proteasome system (Supplementary Fig. S5D) does not affect fitness of cells expressing P > S strong. Finally, we found that the protein disaggregase system (Hsp104, Hsp42, and Hsp26) is not implicated in the tolerance of neither P > S nor R > S misincorporation. Deletion of HSP104 (*Δhsp104*) or combined deletion of HSP104, HSP42, and HSP26 (*Δhsp104*, *Δhsp42*, and *Δhsp26*) did not change the fitness of cells expressing P > S strong or R > S (Fig. 2E and F).

In sum, we show that Hsf1 activity is dispensable for the tolerance of P > S and R > S misincorporation. We also identify the cytosolic Hsp70 chaperone system as the proteostasis system specifically implicated in the tolerance of R > S misincorporation, but not P > S misincorporation.

P > S and R > S misincorporation induce different extents of protein misfolding

It remains unclear whether P > S and R > S misincorporation cause accumulation of misfolded proteins or protein aggregation. We first investigated whether P > S and R > S misincorporation induce the accumulation of polyubiquitinated proteins. To this end, we treated *Δpdr5* cells expressing either vector control, P > S strong, or R > S with 50 μM of the proteasome inhibitor MG-132 for 6 h before lysing cells and performing a western blot. Our data demonstrate that both P > S and R > S misincorporation induce accumulation of polyubiquitinated proteins, which is exacerbated by treatment with MG-132 (Fig. 3A and B). Of note, we observe that only P > S misincorporation leads to the accumulation of insoluble proteins. We fractionated insoluble proteins extracted from cells expressing mistranslating $tRNA^{Ser}$ variants into 2% Triton X-100-soluble (TX+) and -resistant (TX–) fractions. Our data reveal that P > S misincorporation leads to the accumulation of detergent-resistant polyubiquitinated proteins, while R > S misincorporation did not change the solubility of polyubiquitinated proteins (Fig. 3C and D). While R > S misincorporation induced some accumulation of total detergent-resistant proteins, P > S misincorporation induced a much greater accumulation of total detergent-resistant proteins (Fig. 3C and E). We further investigated whether P > S and R > S misincorporation induce protein aggregation using the well-established Hsp104-YFP protein aggregation reporter [24, 51]. We show that neither P > S nor R > S induce an increase in Hsp104-YFP foci formation before or after a heat shock (Fig. 3F and G).

In sum, P > S misincorporation induces that accumulation of detergent-resistant polyubiquitinated proteins, while R > S misincorporation induces accumulation of soluble polyubiquitinated proteins. Notably, neither P > S nor R > S misincorporation induces accumulation of highly insoluble protein aggregates.

R > S misincorporation impairs the association of cytosolic Hsp70 with misfolded proteins

We next explored whether the misfolded proteins that accumulate in mistranslating cells show association with specific molecular chaperones. To this end, we performed sedimentation assays using SSA1-GFP cells to assess whether serine misincorporation changes the solubility of molecular chaperones. We show that both P > S and R > S misincorporation increase the amount of Hsp104 and Hsp42 that co-sediment with insoluble proteins (Fig. 4A–E). However, while P > S misincorporation also increases the amount of Hsp70 that co-sediments with insoluble proteins, R > S misincorporation instead reduces the amount of Hsp70 that co-sediments with insoluble proteins (Fig. 4A–E). We also find profound differences in how P > S and R > S misincorporation change the association of molecular chaperones with 2% Triton X-100-resistant proteins. We find that P > S misincorporation leads to an increase in Hsp42 co-sedimenting with detergent-resistant proteins but induces a decrease in Hsp104 co-sedimenting with detergent-resistant proteins (Fig. 4F–J). In contrast, R > S misincorporation leads to an increase in Hsp104 co-sedimenting with detergent-resistant proteins and leads to a decrease in Hsp70 co-sedimenting with detergent-resistant proteins (Fig. 4F–J). We also used a microscopy-based approach to confirm that R > S misincorporation also induces changes in Hsp70 localization. Using SSA1-GFP cells, we demonstrate that R > S misincorporation increases the formation of Ssa1-GFP foci at 30°C when compared with control cells, likely due to an increase in the distribution of cells containing nuclear Ssa1-GFP (Fig. 4K and L). In addition, after heat shock, cells expressing P > S strong exhibited an increase in Ssa1-GFP foci, whereby Ssa1-GFP formed cytosolic inclusions compared with a predominantly nuclear stain in control cells (Fig. 4K and L).

In sum, both P > S and R > S misincorporation changes the association of molecular chaperones with insoluble proteins. Misfolded proteins caused by P > S misincorporation are mostly associated with Hsp70 and Hsp42. R > S misincorporation, in contrast, prevents Hsp70 association with insoluble proteins plausibly by impairing interactions with Hsp70 and

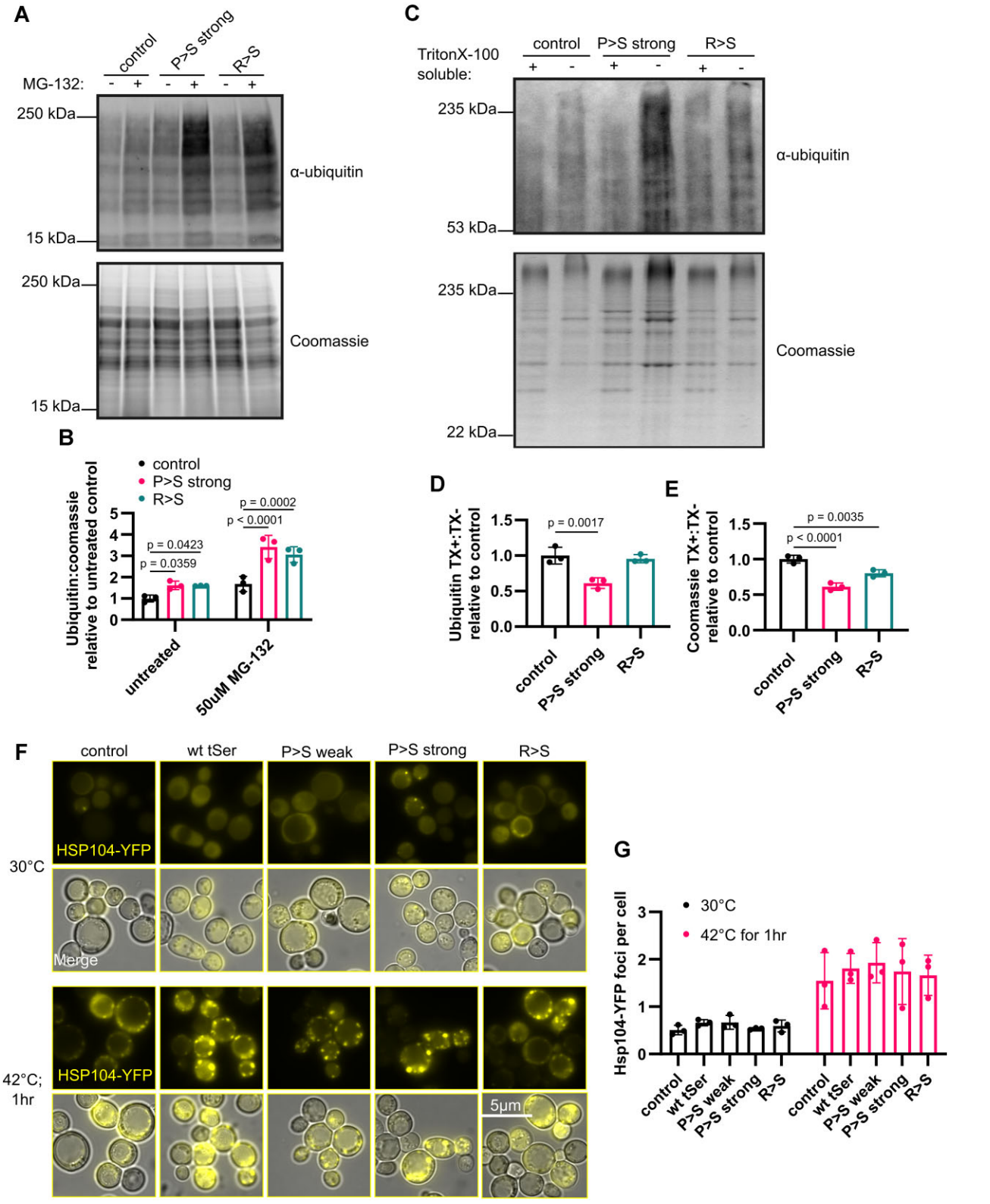

Figure 3. P > S misincorporation induces more accumulation of detergent resistant polyubiquitinated proteins than R > S misincorporation. (**A**) Western blot/Coomassie gel and (**B**) quantification of polyubiquitinated proteins using lysates from cells expressing vector control, P > S strong, or R > S treated with 50 μM MG-132 for 6 h. (**C**) Western blot/Coomassie gel and (**D**, **E**) quantification of proteins in detergent-soluble (TX+) and detergent-resistant (TX–) fractions using lysates from cells expressing either vector control, P > S strong, or R > S. (**F**) Fluorescence microscopy and (**G**) quantification of cells expressing aggregation reporter Hsp104-YFP and either vector control, SUP17 (wt tSer), P > S weak, P > S strong, or R > S before and after heat shock at 42°C for 1 h. The means (±SD) are represented graphically for at least three independent experiments.

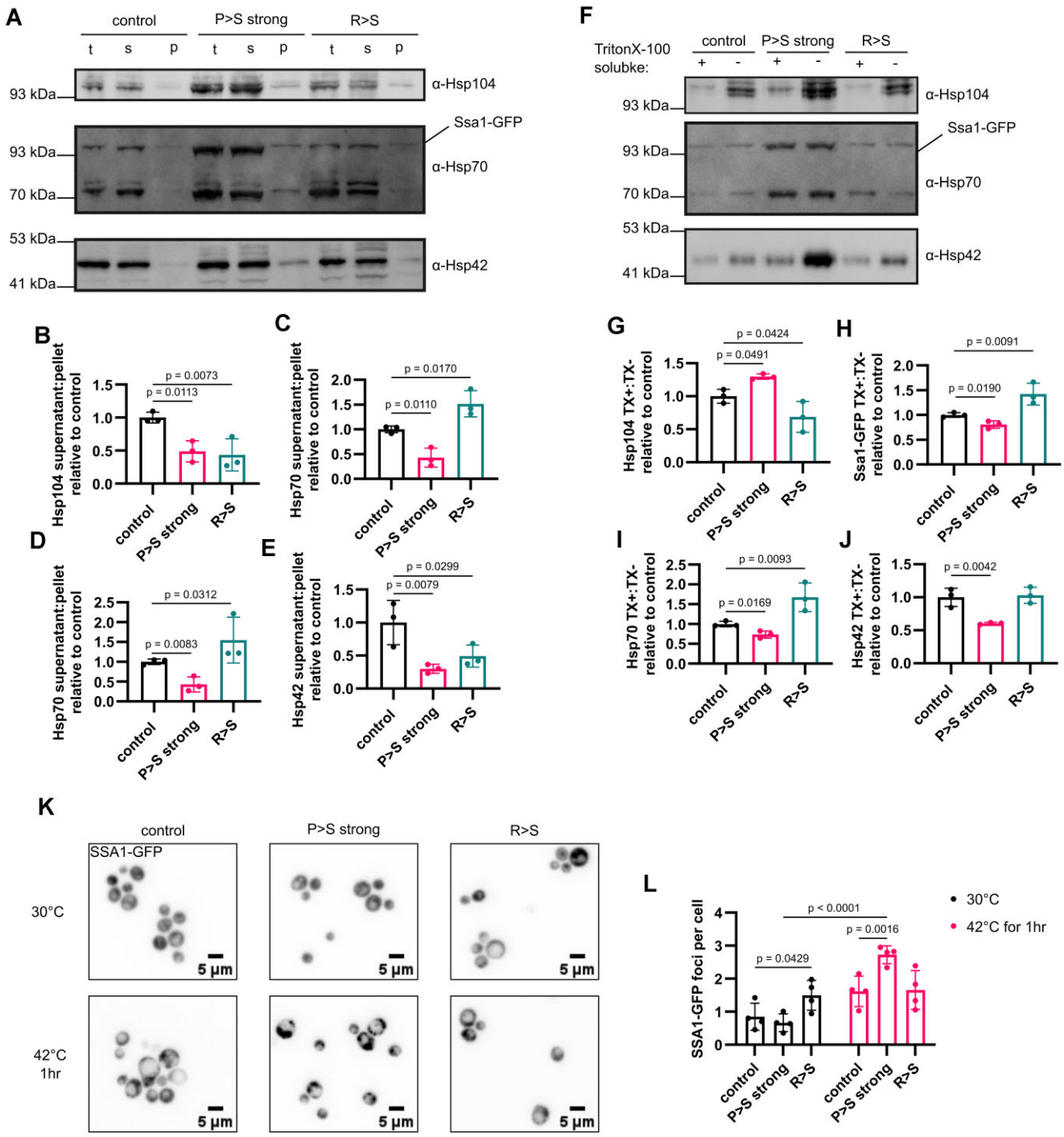

Figure 4. R > S misincorporation reduces Hsp70 association with misfolded proteins. (**A**) Western blot and (**B**–**E**) quantification of sedimented molecular chaperones using lysates from cells expressing either vector control, P > S strong, or R > S. (**F**) Western blot and (**G**–**J**) quantification of molecular chaperones in detergent-soluble (TX+) and detergent-resistant (TX–) protein fractions using lysates from cells expressing either vector control, P > S strong, or R > S. (**K**) Fluorescence microscopy and (**L**) quantification of SSA1-GFP cells expressing either vector control, P > S strong, or R > S before and after a heat shock at 42°C for 1 h. The means (±SD) are represented graphically for at least three independent experiments.

clients containing R > S substitutions (Supplementary Fig. S6) [52–54].

Nascent polypeptide quality control regulates fitness defect caused by P > S misincorporation

While R > S misincorporation seems to impair cytosolic Hsp70s primarily, the specific branch of proteostasis impaired by P > S misincorporation has remained cryptic. We investigated whether P > S and R > S misincorporation impair protein biosynthesis and co-translational protein quality control.

We tested how small molecules that impair translation influence fitness of mistranslating cells. We performed growth assays using agar plates supplemented with the translation inhibitors Hygromycin B, G418, or cycloheximide. We found

that treatment with aminoglycosides, Hygromycin B, and G418, exacerbated the growth defect associated with both P > S strong and R > S (Fig. 5A). Treatment with cycloheximide, however, rescued the growth defect associated with P > S strong and R > S (Fig. 5A). We next tested whether slowing translation by reducing growth temperature influenced tolerance of mistranslating tRNA^{Ser} variants. While growth at 25°C did not change the growth defect associated with P > S strong and R > S, reducing growth temperature to 22°C led to a moderate improvement in the fitness cells expressing P > S strong and R > S when compared with control cells (Fig. 5B).

We again employed genetic tools to uncover the specific molecular chaperones associated with co-translational quality control implicated in tolerance of P > S and R > S misincorporation. Deletion of the nascent polypeptide-associated Hsp70s SSB1 and SSB2 (*Δssb1Δssb2*), the ribosome-associated Hsp70 SSZ1 (*Δssz1*), and all three Hsp70s (*Δssb1Δssb2Δssz1*) all improved fitness of cells expressing\ P > S strong and R > S when compared with control cells (Fig. 5C). We also tested whether impaired degradation of nascent polypeptides influences the fitness of cells expressing mistranslating tRNA^{Ser} variants. Using growth assays, we show that reduced expression of Cdc48 (*DAmP cdc48*) and deletion of the gene encoding Ufd1 (*Δufd1*), both components of a complex involved in the displacement and eventual delivery of polyubiquitinated nascent polypeptides to the proteasome for degradation, reduced the fitness of cells expressing P > S strong, but not R > S (Fig. 5D). We also demonstrate that this interaction is not dependent on ribosome quality control (RQC), as deletion of the genes encoding Asc2, Hel2, Rqc1, and Rqc2 did not change the fitness of cells expressing P > S strong (Supplementary Fig. S7). Furthermore, impaired sorting of nascent polypeptides by the nascent polypeptide-associated complex did not change fitness of cells expressing P > S strong.

In sum, we identify that disrupted protein biosynthesis modulates the fitness defects caused by both P > S and R > S misincorporation. Moreover, we find that degradation of nascent polypeptides specifically regulates the fitness of cells expressing P > S strong, but not the fitness of cells expressing R > S.

P > S mistranslation induces accumulation of nascent polypeptides

Our findings indicate a specific negative interaction between P > S misincorporation and degradation of nascent polypeptides. Using a click chemistry-based approach, we found that only cells expressing P > S strong showed an accumulation of nascent polypeptides when compared with control cells (Fig. 6A and B). We also show the levels of nascent proteins in cells expressing P > S strong undergo delayed degradation compared with control cells. (Fig. 6A and B). As a control, we established that click chemistry labelling is not more efficient in cells expressing P > S strong (Supplementary Fig. S8A and B).

We next tested whether the nascent polypeptides that accumulate in P > S strong cells are responsible for the accumulation of detergent-resistant proteins previously identified. We fractionated the labelled nascent proteins into 2% Triton X-100-soluble (TX+) and -resistant (TX–) fractions. P > S leads to a greater accumulation of total proteins in the detergent-resistant fraction (Fig. 6C and E) and the accumulated nascent proteins caused by P > S misincorporation are mostly detergent-soluble (Fig. 6C and D). As a control we established that click chemistry labelling does not render proteins less resistant to 2% Triton X-100 (Supplementary Fig. S8C and D).

To complement our prior findings that nascent polypeptides accumulate in cells expressing P > S strong, we used an alternative labelling approach to measure nascent polypeptides levels. Validating our prior findings, we confirm that *Δpdr5* cells expressing P > S strong accumulated more puromycin-labelled nascent polypeptide chains than control cells (Fig. 6F and G). Notably, the amount of puromycin-labelled nascent polypeptide chains in reduced by ∼50% after removing the puromycin for 5 min, independent of P > S misincorporation (Fig. 6F and G). We immunoprecipitated puromycin-labelled nascent proteins to investigate whether the accumulation of nascent polypeptides is due to a defect in polyubiquitination of nascent proteins. Our data reveal an increase in levels of ubiquitinated puromycin-labelled nascent polypeptides in cells expressing P > S strong (Fig. 6H and I).

In sum, we show that P > S misincorporation induces the accumulation of soluble, polyubiquitinated nascent polypeptides. While these nascent polypeptides are not resistant to detergents, our findings indicate that the accumulation of soluble nascent polypeptides precedes the accumulated detergent-resistant polyubiquitinated proteins.

Discussion

The Hsp70 chaperone system regulates tolerance of R > S misincorporation

Mistranslating tRNA variants are highly prevalent in the human population [16] and can be detrimental to cellular fitness [4, 8, 10, 11, 19, 21]. Although many mistranslating tRNA variants impair proteostasis, induce cellular stress responses, and cause protein aggregation, it remains unclear how proteostasis regulates the detrimental effects of specific mistranslating tRNAs [4, 5, 7, 8, 11]. Confounding this problem, the severity and the specific interactions with proteostasis depend on the type of amino acid misincorporation and even the specific mistranslated codon [9, 12, 13]. To study such a complex problem, we employ yeast as a model system optimally suited to quantitatively assess how proteostasis regulates the fitness of cells expressing different mistranslating tRNAs. We show that two different mistranslating tRNA^{Ser} variants, one mistranslating proline codons to serine (P > S) and the other mistranslating arginine codons to serine (R > S), challenge proteostasis by inducing the accumulation of misfolded proteins. Remarkably, we find that even though both mistranslating tRNAs induce serine misincorporation, they interact with distinct branches of the proteostasis network to impair cellular fitness.

Mistranslating tRNA^{Ser} variants can induce several stress responses, such as the general stress response in yeast [11], the unfolded protein response in human cells [7], in mouse tumors [6], and in chick [22] and zebrafish embryos [8], and the heat shock response in zebrafish embryos [8]. Here, we find that the constitutive expression of mistranslating tRNA^{Ser} variants that cause P > S and R > S misincorporation impairs the growth of yeast cells, particularly under protein misfolding stress, and induces the heat shock response as detected by increased protein levels of Ssa1, Hsp104, and Hsp42. Notably, P > S misincorporation induces a stronger growth

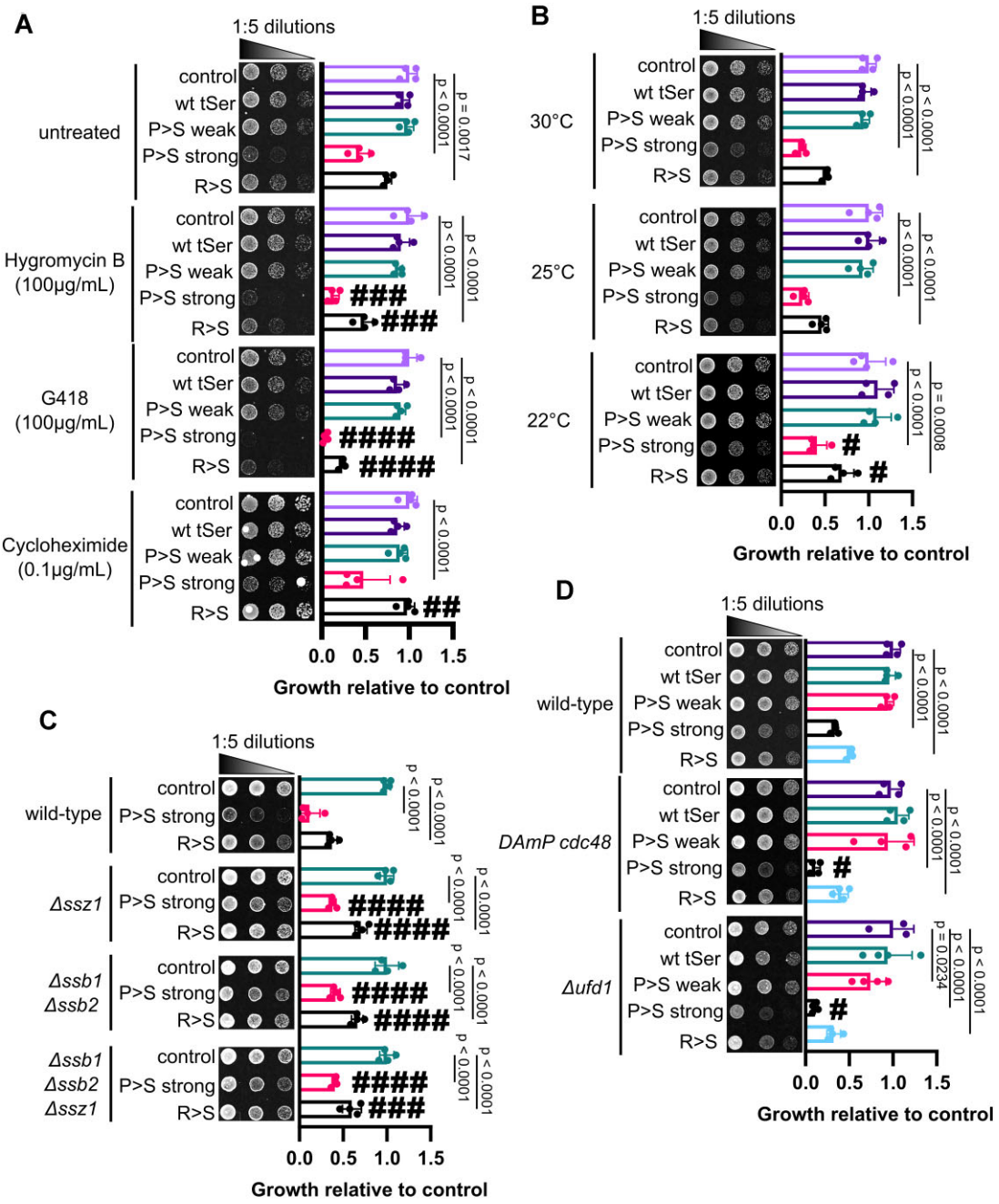

Figure 5. Impaired degradation of nascent polypeptides sensitizes cells to P > S misincorporation. (**A**) Growth assays of cells expressing either vector control, wild-type SUP17 (wt tSer), or the SUP17 variants P > S weak, P > S strong, or R > S at 30°C, 25°C, or at 22°C. (**B**) Growth assays of cells expressing either vector control, wt tSer, P > S weak, P > S strong, or R > S on plates supplemented with either Hygromycin B, G418, or cycloheximide. (**C**) Growth assays of *Δssz1*, *Δssb1Δssb2*, or *Δssb1Δssb2Δssz1* cells expressing either vector control, P > S strong, or R > S. (**D**) Growth assays with *DAmP cdc48* or *Δufd1* cells expressing either vector control, wt tSer, P > S weak, P > S strong, or R > S. The mean growth (±SD) relative to vector control is represented graphically for at least three independent experiments. # Symbols indicate significant differences compared with wild-type cells expressing the same tRNA variant in control conditions (*#P* < .05; *##P* < .01; *###P* < .001; *####P* < .0001).

defect and greater heat shock response than R > S despite similar rates of mistranslation (5% and 3.5%, respectively) [5, 13]. We conclude that changes of proline residues by mistranslation introduce a greater burden on proteostasis than changes of arginine residues. Accordingly, exposure to the proline analogue, azetidine-2-carboxylic acid, induces a potent heat shock response, while treatment with the arginine analogue, canavanine, does not [55]. The expression of both P > S and R > S mistranslating $tRNA^{Ser}$ variants induce proteostasis genes that are regulated by the stress responsive transcription factors Hsf1, Msn2, and Msn4. Yet, neither cells expressing P > S nor R > S mistranslating $tRNA^{Ser}$ variants were sensitive to oxidative stress and endoplasmic reticulum stress, demonstrating selective interactions with cytoplasmic proteostasis stress. Similarly, treatment with azetidine-2-carboxylic acid induces genes regulated by Hsf1, Msn2, and Msn4, but not the ER stress responsive Hac1, suggesting that cells are competent to tolerate mistranslated proteins in the ER [55].

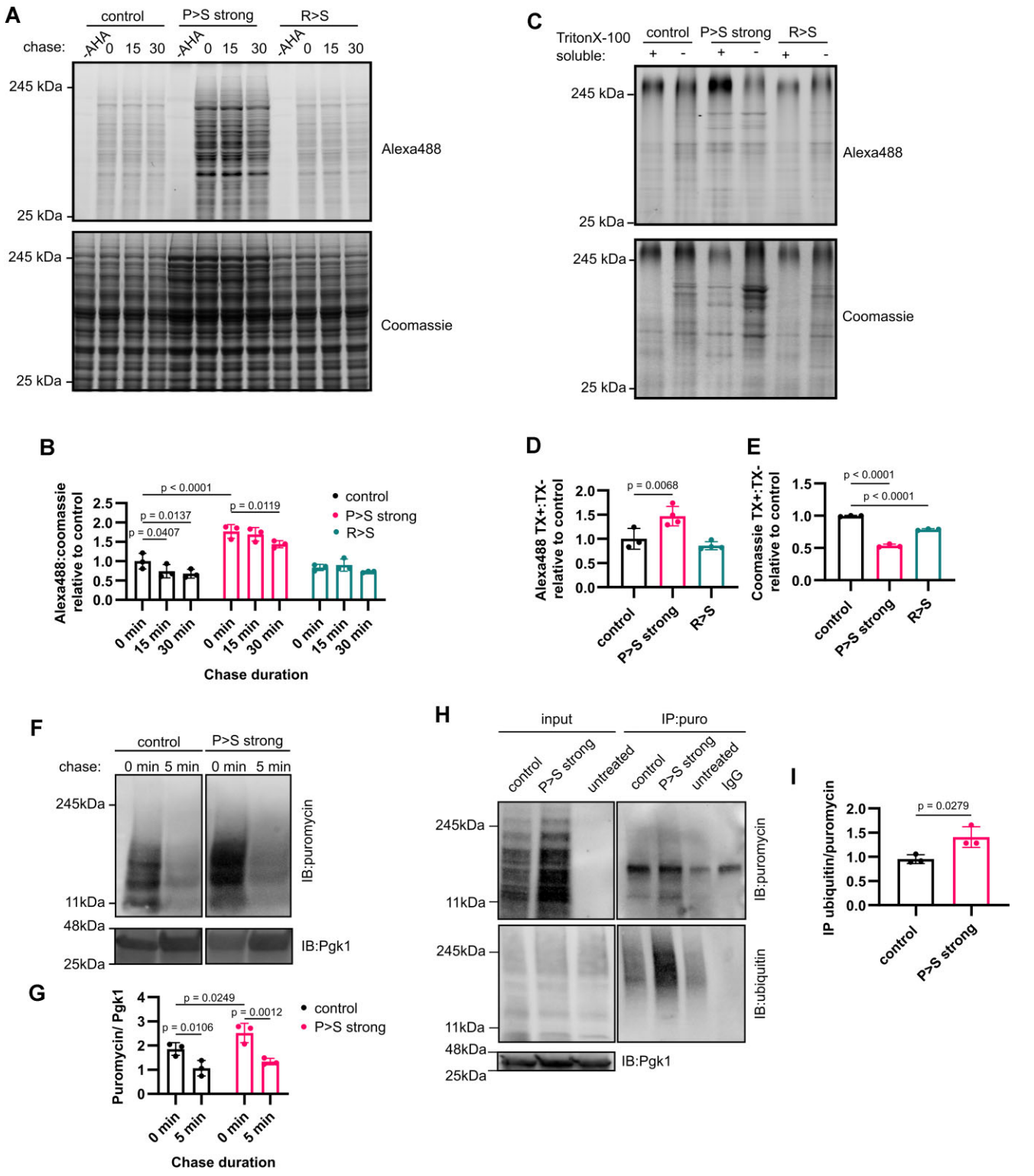

Figure 6. P > S, but not R > S, misincorporation induces accumulation of nascent polypeptides. (**A**) SDS–PAGEs and (**B**) quantification of 5-min SPAAC pulse chase of nascent proteins using lysates from cells expressing either vector control, P > S strong, or R > S. (**C**) SDS–PAGEs and (**D**, **E**) quantification of 5-min labelled nascent proteins in detergent-soluble (TX+) and detergent-resistant (TX–) protein fractions using lysates from cells expressing either vector control, P > S strong, or R > S. (**F**) Western blot and (**G**) quantification of 5-min puromycin pulse chase of nascent proteins using lysates from cells expressing either vector control or P > S strong. (**H**) Immunoprecipitation of puromycin labelled nascent proteins and (**I**) quantification of polyubiquinated nascent proteins using lysates from cells expressing either vector control or P > S strong. The means (±SD) are represented graphically for at least three independent experiments.

We show that although mistranslating $tRNA^{Ser}$ variants induce the heat shock response, Hsf1 activation is insufficient to improve cellular fitness. Increasing Hsf1 activity did not improve the fitness of mistranslating cells, whereas reducing Hsf1 activity, surprisingly, improved fitness. We therefore speculated that molecular chaperones expressed under basal conditions, rather than those induced by stress, predominantly mitigate the growth defect caused by mistranslation.

Molecular chaperones and protein remodeling factors generally mitigate the negative effects of protein misfolding caused by proteostasis stress. Of note, however, our systematic genetic analyses demonstrated that Hsp70 uniquely counteracts the negative effects of mistranslation, whereas Hsp90, Hsp104, and small heat shock proteins did not. Specifically, we find that depletion of Hsp70 and the Hsp70 co-chaperone Sis1, exacerbated the fitness defect associated with R > S misincorporation, particularly under stress conditions. Hsp70 requires positively charged residues to recognize and interact with client proteins [52, 53]. Therefore, R > S mistranslation may directly impair Hsp70–client interactions. Also, Sis1 binds misfolded clients, prevents their aggregation, and possibly acts as a scaffold to recruit Hsp70 to refold misfolded proteins [56]. Sis1 may compensate for the impaired interactions between Hsp70 and misfolded peptides containing R > S amino acid substitutions. Our data thus unravel a plausible mechanism by which proteins with R > S amino acid substitutions evade chaperoning by Hsp70 due to impaired binding of Hsp70 to mistranslated substrates. By contrast, P > S misincorporation appears less reliant on cytosolic Hsp70.

Hsp70 dysfunction and protein misfolding in mistranslating cells

P > S and R > S misincorporation both induced accumulation of polyubiquitinated proteins, albeit to different degrees. P > S and R > S misincorporation induced accumulation of detergent-resistant proteins, although their biophysical properties depend on the type of mistranslation. P > S misincorporation strongly promotes accumulation of detergent-resistant polyubiquitinated proteins. By contrast, R > S only moderately promotes accumulation of detergent-resistant polyubiquitinated proteins. Although both P > S and R > S induce the accumulation of proteins that resist solubilization by mild detergents, we have little evidence to suggest they form aggregates, as they do not recruit Hsp104 into the cellular inclusions typical of aggregates. In parallel to the different properties of accumulated proteins, P > S and R > S misincorporation also determine the association of different molecular chaperones. Detergent-resistant proteins induced by P > S misincorporation are primarily associated with Hsp42 and Hsp70 and induce the formation of Hsp70 cytosolic inclusions in cells exposed to heat shock. By contrast, detergent-resistant proteins induced by R > S misincorporation associate with Hsp104 but only little with Hsp70 and Hsp42. In agreement with our genetic findings, we deduce that the accumulation of detergent-resistant proteins caused by R > S misincorporation primarily results from the reduced ability of Hsp70 to bind mistranslated proteins (Fig. 7B). We additionally speculate that loss of arginine residues in disease-associated protein variants can similarly evade detection by Hsp70, plausibly compounding their misfolding and/or aggregation. In contrast, the accumulation of detergent-resistant proteins caused by P > S misincorporation is plausibly caused by the misfolding of mistranslated peptides due to the formation of aberrant alpha helices due to the loss of prolines that disrupt alpha helix formation and promote structural integrity [57, 58].

Accumulation of nascent polypeptides in mistranslating cells

Previous studies indicate that serine misincorporation impairs translation [19, 21] and prevents proper polysome assembly [11]. Our genetic and biochemical experiments determined that P > S misincorporation induced the accumulation of nascent polypeptides (Fig. 7A). Typically, nascent polypeptides are rapidly degraded when ribosomes stall through a process called RQC [59]. Other studies detected polyubiquitinated substrates associated with the 80S ribosome, particularly when the Cdc48/Npl4/Ufd1 complex is impaired [60–62]. We do not detect a genetic interaction between RQC and mistranslation; however, depletion of Cdc48 and Ufd1 sensitizes cells to P > S misincorporation but not R > S. We, thus, demonstrate that impaired degradation of nascent proteins contributes to growth defects caused by P > S misincorporation, which is partially mitigated by the Cdc48/Npl4/Ufd1 complex.

The ribosome-associated Hsp70s, Ssb1, Ssb2, and Ssz1, participate in degradation of nascent polypeptides [60]. We show that depletion of ribosome-associated Hsp70s, which reduces the number of polysomes, rescues the detrimental effects of both P > S and R > S misincorporation. Further mechanistic studies are required to assess how exactly ribosome-associated Hsp70s regulate protein quality control of mistranslated nascent polypeptides. We also establish a nexus between compromised translation fidelity and the misfolding of *de novo* translated proteins. Specifically, we find that P > S misincorporation results in the accumulation of soluble polyubiquitinated, nascent polypeptides. Despite causing the accumulation of polyubiquitinated nascent polypeptides, P > S misincorporation does not interact genetically with impaired function of the ubiquitin proteasome system. We speculate that Cdc48/Npl4/Ufd1 complex, not the 26S proteasome itself, is overwhelmed by the accumulation of nascent polypeptides, preventing their timely degradation. Of note, R > S misincorporation does not interact with proteostasis of nascent proteins at the ribosome, suggesting that mistranslation of arginine selectively impairs proteostasis post-translationally. By contrast, we conclude that mistranslation of proline is oppressive to co-translational proteostasis, and may promote a cascade of post-translational proteostasis defects.

Conclusion

Over 10% of human tRNA genes vary from the standard genetic code [16]. Many of these tRNA variants challenge protein homeostasis (proteostasis) by erroneously translating mRNA codons into amino acids (mistranslation). While many mistranslating tRNA variants impair cellular fitness by inducing protein misfolding [8, 11, 22], some are well tolerated [18], prevent disease-associated protein aggregation [19, 21], and are even being considered as potential therapeutics [20]. Understanding the specific mechanisms by which different mistranslating tRNA variants affect proteostasis is crucial. We show that different types of mistranslation have distinct outcomes on cellular fitness, result in distinct accumulation of

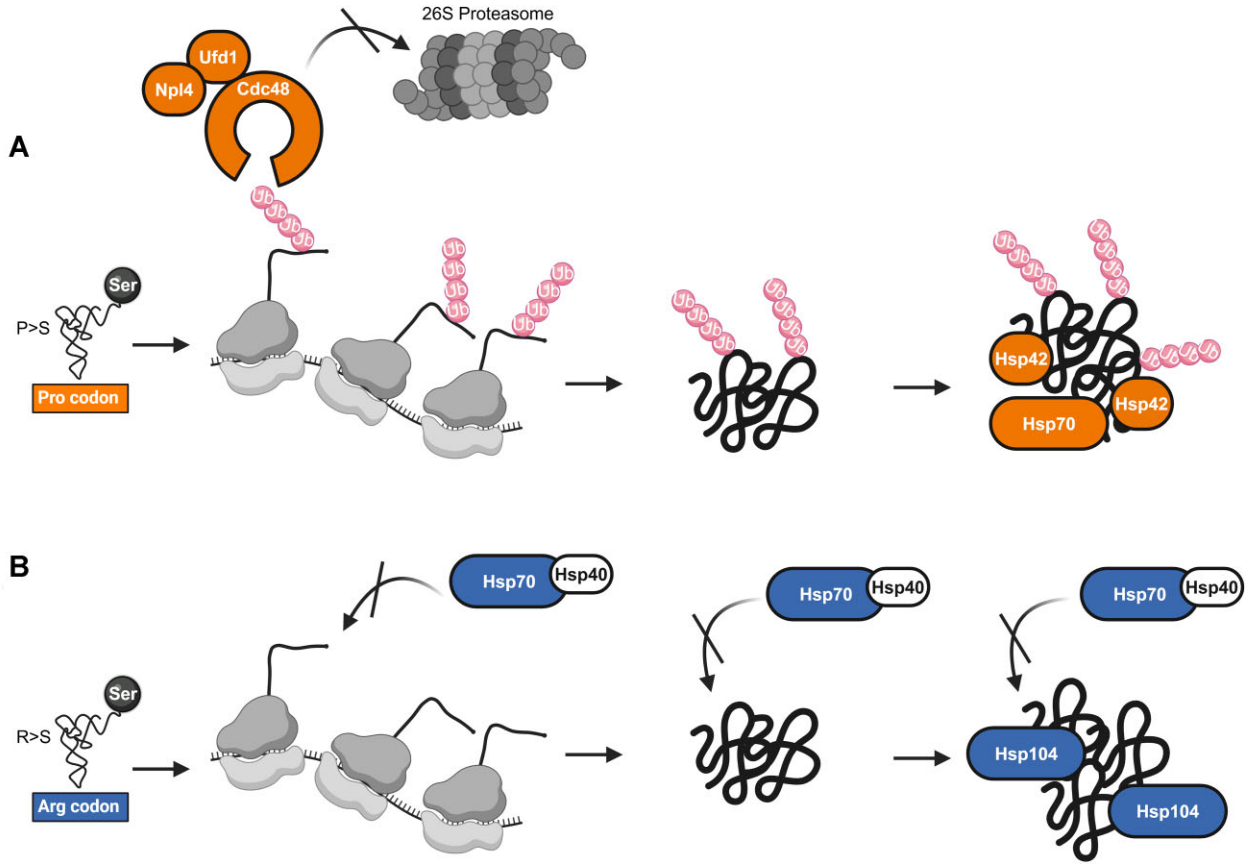

Figure 7. Schematic summary of the proteostasis systems impaired by mistranslating $tRNA^{Ser}$ variants. (**A**) P > S misincorporation induces the accumulation of nascent polypeptides which overwhelm the Cdc48/Npl4/Ufd1 complex, impairing their degradation by the ubiquitin proteasome system. The accumulated nascent polypeptides are ubiquitinated and accumulate as detergent-soluble, possibly misfolded states before eventually forming detergent-resistant complexes that associate with Hsp70 and Hsp42. (**B**) R > S misincorporation yields the production of mistranslated nascent polypeptides that evade protein quality control by Hsp70, exacerbating their misfolding post-translationally. These mistranslated peptides eventually form detergent-resistant complexes that predominantly associate with Hsp104.

misfolded proteins, and interact with distinct branches of proteostasis. Specifically, R > S misincorporation impairs interactions between Hsp70 and misfolded proteins, while P > S misincorporation impairs degradation of nascent proteins. Taken together, our findings highlight the unexpected specificity by which mistranslation affects proteostasis and cellular fitness.

Acknowledgements

We would like to thank Drs Christopher J. Brandl (University of Western Ontario, Emeritus), David Pincus (University of Chicago), Elke Deuerling (University of Konstanz), and Elizabeth Craig (University of Wisconsin-Madison) and Johannes Buchner (Technical University of Munich) for providing plasmids, yeast strains and antibodies for this study. We would also like to thank Drs Christopher J. Brandl, Matthew Berg (University of Washington), Maria Vera-Ugalde (McGill University), Paul Walton (University of Western Ontario), and Patrick Lajoie (University of Western Ontario) for critical reading of the manuscript. We would also like to thank Benjamin S. Rutledge for his assistance providing the graph of the crystal structure of DnaK bound to a model substrate. All schematics were produced using BioRender.

Author contributions: Donovan W. McDonald (Investigation, Conceptualization, Formal analysis, Methodology, Supervision, Validation, Visualization, Writing—original draft, Writing—review & editing), Rebecca N. Dib (Investigation, Formal analysis, Methodology), Christopher De Luca (Investigation, Formal analysis), Ashmi Shah (Investigation), and Martin L. Duennwald (Conceptualization, Funding acquisition, Project administration, Resources, Supervision, Writing—review & editing)

Supplementary data

Supplementary data is available at NAR online.

Conflict of interest

We have no conflicts of interest to declare.

Funding

Funding for this research was provided by an NSERC Discovery grant (RGPIN-2024-05867) and a McGill-Western Initiative for Translational Neuroscience (ITN) grant to M.L.D., and an ALS Canada Trainee Fellowship to D.W.M. This research was also supported by CIHR Skin Research Training Centre (201903). Funding to pay the Open Access publication charges for this article was provided by: ITN grant to M.L.D.

Data availability

R script for analysis of fluorescence microscopy is available at https://doi.org/10.6084/m9.figshare.28688966. FASTQ files with RNA sequencing data from cells expressing either vector control, P > S strong or R > S were acquired from NCBI Gene Expression Omnibus series accession number GSE174145. The crystal structure of DnaK and a model substrate were acquired from Protein Data Bank with accession code 4R5I.

References

1. Berg MD, Brandl CJ. Transfer RNAs: diversity in form and function. *Nucleic Acids Res* 2021;**18**:6840–52. https://doi.org/10.1080/15476286.2020.1809197
2. Kramer EB, Vallabhaneni H, Mayer LM *et al.* A comprehensive analysis of translational missense errors in the yeast *Saccharomyces cerevisiae*. *RNA* 2010;**16**:1797–808. https://doi.org/10.1261/rna.2201210
3. Giegé R, Eriani G. The tRNA identity landscape for aminoacylation and beyond. *Nucleic Acids Res* 2023;**51**:1528–70. https://doi.org/10.1093/nar/gkad007
4. Berg MD, Hoffman KS, Genereaux J *et al.* Evolving mistranslating tRNAs through a phenotypically ambivalent intermediate in *Saccharomyces cerevisiae*. *Genetics* 2017;**206**:1865–79. https://doi.org/10.1534/genetics.117.203232
5. Berg MD, Zhu Y, Genereaux J *et al.* Modulating mistranslation potential of tRNASer in *Saccharomyces cerevisiae*. *Genetics* 2019;**213**:849–63. https://doi.org/10.1534/genetics.119.302525
6. Santos M, Pereira PM, Varanda AS *et al.* Codon misreading tRNAs promote tumor growth in mice. *RNA Biol* 2018;**15**:773–86.
7. Varanda AS, Santos M, Soares AR *et al.* Human cells adapt to translational errors by modulating protein synthesis rate and protein turnover. *RNA Biol* 2020;**17**:135–49. https://doi.org/10.1080/15476286.2019.1670039
8. Reverendo M, Soares AR, Pereira PM *et al.* TRNA mutations that affect decoding fidelity deregulate development and the proteostasis network in zebrafish. *RNA Biol* 2014;**11**:1199–213. https://doi.org/10.4161/rna.32199
9. Isaacson JR, Berg MD, Jagiello J *et al.* Mistranslating tRNA variants have anticodon- and sex-specific impacts on *Drosophila melanogaster*. *G3 (Bethesda)* 2024;**14**:jkae230. https://doi.org/10.1093/g3journal/jkae230
10. Isaacson JR, Berg MD, Charles B *et al.* A novel mistranslating tRNA model in *Drosophila melanogaster* has diverse, sexually dimorphic effects. *G3 (Bethesda)* 2022;**12**:jkac035.
11. Paredes JA, Carreto L, Simões J *et al.* Low level genome mistranslations deregulate the transcriptome and translatome and generate proteotoxic stress in yeast. *BMC Biol* 2012;**10**:55. https://doi.org/10.1186/1741-7007-10-55
12. Cozma E, Rao M, Dusick M *et al.* Anticodon sequence determines the impact of mistranslating tRNAAla variants. *RNA Biol* 2023;**20**:791–804. https://doi.org/10.1080/15476286.2023.2257471
13. Berg MD, Zhu Y, Ruiz BY *et al.* The amino acid substitution affects cellular response to mistranslation. *G3 (Bethesda)* 2021;**11**:jkab218.
14. Lant JT, Berg MD, Sze DHW *et al.* Visualizing tRNA-dependent mistranslation in human cells. *RNA Biol* 2018;**15**:567–75. https://doi.org/10.1080/15476286.2017.1379645
15. Hoffman KS, Berg MD, Shilton BH *et al.* Genetic selection for mistranslation rescues a defective co-chaperone in yeast. *Nucleic Acids Res* 2017;**45**:3407–21. https://doi.org/10.1093/nar/gkw1021
16. Berg MD, Giguere DJ, Dron JS *et al.* Targeted sequencing reveals expanded genetic diversity of human transfer RNAs. *RNA Biol* 2019;**16**:1574–85. https://doi.org/10.1080/15476286.2019.1646079
17. Berg MD, Zhu Y, Loll-Krippleber R *et al.* Genetic background and mistranslation frequency determine the impact of mistranslating tRNASerUGG. *G3 (Bethesda)* 2022;**12**:jkac125. https://doi.org/10.1093/g3journal/jkac125
18. Hasan F, Lant JT, O'Donoghue P. Perseverance of protein homeostasis despite mistranslation of glycine codons with alanine. *Philos Trans R Soc Lond B Biol Sci* 2023;**378**:20220029. https://doi.org/10.1098/rstb.2022.0029
19. Lant JT, Kiri R, Duennwald ML *et al.* Formation and persistence of polyglutamine aggregates in mistranslating cells. *Nucleic Acids Res* 2021;**49**:11883–99. https://doi.org/10.1093/nar/gkab898
20. Hou Y, Zhang W, McGilvray PT *et al.* Engineered mischarged transfer RNAs for correcting pathogenic missense mutations. *Mol Ther* 2024;**32**:352–71. https://doi.org/10.1016/j.ymthe.2023.12.014
21. Lant JT, Hasan F, Briggs J *et al.* Genetic interaction of tRNA-dependent mistranslation with fused in sarcoma protein aggregates. *Genes (Basel)* 2023;**14**:518. https://doi.org/10.3390/genes14020518
22. Geslain R, Cubells L, Bori-Sanz T *et al.* Chimeric tRNAs as tools to induce proteome damage and identify components of stress responses. *Nucleic Acids Res* 2010;**38**:e30. https://doi.org/10.1093/nar/gkp1083
23. Berg MD, Isaacson JR, Cozma E *et al.* Regulating expression of mistranslating tRNAs by Readthrough RNA polymerase II transcription. *ACS Synth Biol* 2021;**10**:3177–89.
24. Tavares JF, Davis NK, Poim A *et al.* tRNA-modifying enzyme mutations induce codon-specific mistranslation and protein aggregation in yeast. *RNA Biol* 2021;**18**:563–75. https://doi.org/10.1080/15476286.2020.1819671
25. Hipp MS, Kasturi P, Hartl FU. The proteostasis network and its decline in ageing. *Nat Rev Mol Cell Biol* 2019;**20**:421–35. https://doi.org/10.1038/s41580-019-0101-y
26. Rutledge BS, Choy W-Y, Duennwald ML. Folding or holding?—Hsp70 and Hsp90 chaperoning of misfolded proteins in neurodegenerative disease. *J Biol Chem* 2022;**298**:101905. https://doi.org/10.1016/j.jbc.2022.101905
27. Winkler J, Tyedmers J, Bukau B *et al.* Chaperone networks in protein disaggregation and prion propagation. *J Struct Biol* 2012;**179**:152–60. https://doi.org/10.1016/j.jsb.2012.05.002
28. Zheng X, Krakowiak J, Patel N *et al.* Dynamic control of Hsf1 during heat shock by a chaperone switch and phosphorylation. *eLife* 2016;**5**:e18638. https://doi.org/10.7554/eLife.18638
29. Krakowiak J, Zheng X, Patel N *et al.* Hsf1 and Hsp70 constitute a two-component feedback loop that regulates the yeast heat shock response. *eLife* 2018;**7**:e31668. https://doi.org/10.7554/eLife.31668
30. Gautschi M, Lilie H, Fünfschilling U *et al.* RAC, a stable ribosome-associated complex in yeast formed by the DnaK–DnaJ homologs Ssz1p and zuotin. *Proc Natl Acad Sci USA* 2001;**98**:3762–7. https://doi.org/10.1073/pnas.071057198
31. Brandman O, Stewart-Ornstein J, Wong D *et al.* A ribosome-bound quality control complex triggers degradation of nascent peptides and signals translation stress. *Cell* 2012;**151**:1042–54. https://doi.org/10.1016/j.cell.2012.10.044
32. George R, Beddoe T, Landl K *et al.* The yeast nascent polypeptide-associated complex initiates protein targeting to mitochondria *in vivo*. *Proc Natl Acad Sci USA* 1998;**95**:2296–301. https://doi.org/10.1073/pnas.95.5.2296
33. Pincus D, Chevalier MW, Aragón T *et al.* BiP binding to the ER-stress sensor Ire1 tunes the homeostatic behavior of the unfolded protein response. *PLoS Biol* 2010;**8**:e1000415. https://doi.org/10.1371/journal.pbio.1000415
34. Cashikar AG, Duennwald M, Lindquist SL. A chaperone pathway in protein disaggregation: Hsp26 alters the nature of protein aggregates to facilitate reactivation by Hsp104. *J Biol Chem* 2005;**280**:23869–75. https://doi.org/10.1074/jbc.M502854200

35. Rutledge BS, Kim YJ, McDonald DW *et al.* Stress-inducible phosphoprotein 1 (Sti1/Stip1/Hop) sequesters misfolded proteins during stress. *FEBS J* 2024. https://doi.org/10.1111/febs.17389
36. Schilke BA, Ciesielski SJ, Ziegelhoffer T *et al.* Broadening the functionality of a J-protein/Hsp70 molecular chaperone system. *PLoS Genet* 2017;**13**:e1007084. https://doi.org/10.1371/journal.pgen.1007084
37. Lee K, Ziegelhoffer T, Delewski W *et al.* Pathway of Hsp70 interactions at the ribosome. *Nat Commun* 2021;**12**:5666. https://doi.org/10.1038/s41467-021-25930-8
38. Koplin A, Preissler S, Ilina Y *et al.* A dual function for chaperones SSB–RAC and the NAC nascent polypeptide–associated complex on ribosomes. *J Cell Biol* 2010;**189**:57–68. https://doi.org/10.1083/jcb.200910074
39. Giaever G, Chu AM, Ni L *et al.* Functional profiling of the *Saccharomyces cerevisiae* genome. *Nature* 2002;**418**:387–91. https://doi.org/10.1038/nature00935
40. Huh W-K, Falvo JV, Gerke LC *et al.* Global analysis of protein localization in budding yeast. *Nature* 2003;**425**:686–91. https://doi.org/10.1038/nature02026
41. Breslow DK, Cameron DM, Collins SR *et al.* A comprehensive strategy enabling high-resolution functional analysis of the yeast genome. *Nat Methods* 2008;**5**:711–8. https://doi.org/10.1038/nmeth.1234
42. Gietz RD, Schiestl RH. High-efficiency yeast transformation using the LiAc/SS carrier DNA/PEG method. *Nat Protoc* 2007;**2**:31–4. https://doi.org/10.1038/nprot.2007.13
43. Chee MK, Haase SB. New and redesigned pRS Plasmid Shuttle vectors for genetic manipulation of *Saccharomyces cerevisiae*. *G3 (Bethesda)* 2012;**2**:515–26. https://doi.org/10.1534/g3.111.001917
44. Petropavlovskiy AA, Tauro MG, Lajoie P *et al.* A quantitative imaging-based protocol for yeast growth and survival on agar plates. *STAR Protoc* 2020;**1**:100182. https://doi.org/10.1016/j.xpro.2020.100182
45. Schindelin J, Arganda-Carreras I, Frise E *et al.* Fiji: an open-source platform for biological-image analysis. *Nat Methods* 2012;**9**:676–82. https://doi.org/10.1038/nmeth.2019
46. von der Haar T. Optimized protein extraction for quantitative proteomics of yeasts. *PLoS One* 2007;**2**:e1078. https://doi.org/10.1371/journal.pone.0001078
47. Abdulrehman D, Monteiro PT, Teixeira MC *et al.* YEASTRACT: providing a programmatic access to curated transcriptional regulatory associations in *Saccharomyces cerevisiae* through a web services interface. *Nucleic Acids Res* 2011;**39**:D136–40. https://doi.org/10.1093/nar/gkq964
48. Pau G, Fuchs F, Sklyar O *et al.* EBImage—an R package for image processing with applications to cellular phenotypes. *Bioinformatics* 2010;**26**:979–81.
49. Morey TM, Esmaeili MA, Duennwald ML *et al.* SPAAC pulse-chase: a novel click chemistry-based method to determine the half-life of cellular proteins. *Front Cell Dev Biol* 2021;**9**:722560. https://doi.org/10.3389/fcell.2021.722560
50. Hartl FU. Molecular chaperones in cellular protein folding. *Nature* 1996;**381**:571–9. https://doi.org/10.1038/381571a0
51. Lum R, Tkach JM, Vierling E *et al.* Evidence for an unfolding/threading mechanism for protein disaggregation by *Saccharomyces cerevisiae* Hsp104. *J Biol Chem* 2004;**279**:29139–46. https://doi.org/10.1074/jbc.M403777200
52. Zhu X, Zhao X, Burkholder WF *et al.* Structural analysis of substrate binding by the molecular chaperone DnaK. *Science* 1996;**272**:1606–14. https://doi.org/10.1126/science.272.5268.1606
53. Rüdiger S, Germeroth L, Schneider-Mergener J *et al.* Substrate specificity of the DnaK chaperone determined by screening cellulose-bound peptide libraries. *EMBO J* 1997;**16**:1501–7. https://doi.org/10.1093/emboj/16.7.1501
54. Leu JI-J, Zhang P, Murphy ME *et al.* Structural basis for the inhibition of HSP70 and DnaK chaperones by small-molecule targeting of a C-terminal allosteric pocket. *ACS Chem Biol* 2014;**9**:2508–16. https://doi.org/10.1021/cb500236y
55. Trotter EW, Kao CM-F, Berenfeld L *et al.* Misfolded proteins are competent to mediate a subset of the responses to heat shock in *Saccharomyces cerevisiae*. *J Biol Chem* 2002;**277**:44817–25. https://doi.org/10.1074/jbc.M204686200
56. Klaips CL, Gropp MHM, Hipp MS *et al.* Sis1 potentiates the stress response to protein aggregation and elevated temperature. *Nat Commun* 2020;**11**:6271. https://doi.org/10.1038/s41467-020-20000-x
57. Piela L, Némethy G, Scheraga HA. Proline-induced constraints in α-helices. *Biopolymers* 1987;**26**:1587–600. https://doi.org/10.1002/bip.360260910
58. O'Neil KT, DeGrado WF. A thermodynamic scale for the helix-forming tendencies of the commonly occurring amino acids. *Science* 1990;**250**:646–51.
59. Sitron CS, Brandman O. Detection and degradation of stalled nascent chains via ribosome-associated quality control. *Annu Rev Biochem* 2020;**89**:417–42. https://doi.org/10.1146/annurev-biochem-013118-110729
60. Ghosh A, Shcherbik N. Cooperativity between the ribosome-associated chaperone Ssb/RAC and the ubiquitin ligase Ltn1 in ubiquitination of nascent polypeptides. *Int J Mol Sci* 2020;**21**:6815. https://doi.org/10.3390/ijms21186815
61. Verma R, Oania RS, Kolawa NJ *et al.* Cdc48/p97 promotes degradation of aberrant nascent polypeptides bound to the ribosome. *eLife* 2013;**2**:e00308. https://doi.org/10.7554/eLife.00308
62. Shcherbik N, Chernova TA, Chernoff YO *et al.* Distinct types of translation termination generate substrates for ribosome-associated quality control. *Nucleic Acids Res* 2016;**44**:6840–52. https://doi.org/10.1093/nar/gkw566

Received: February 4, 2025. **Revised:** April 16, 2025. **Editorial Decision:** April 16, 2025. **Accepted:** May 7, 2025